A study on the energy transfer of a square prism under aeroelastic galloping

H.G.K.G. Jayatunga, B.T. Tan, J. S. Leontini

Abstract

Extracting useful energy from flow induced vibrations has become a developing area of research in recent years. In this paper, we analyse power transfer of an elastically mounted body under the influence of aeroelastic galloping. The system and the power transfer is analysed by numerically integrating the quasi-steady state model equations. The power transfer is analysed for both high ($Re = 22300$) and low ($Re = 165$) Reynolds numbers cases, and the impact of the system mass is investigated for both.

At high mass ratios ($m^* > 50$), the power transfer is completely controlled by galloping and essentially independent of the mass. A combined mass-damping coefficient, Π_2, that can be derived from the equation of motion, is shown to be the parameter that governs power output. The system is a balance between the power delivered to the system due to hydrodynamic forcing and power removed through mechanical damping which are governed by the hydrodynamic forcing characteristics (i.e. the lift force as a function of incident angle) and mechanical damping coefficient respectively. The peak efficiency of 0.26% for $Re = 165$ and 6.7% for $Re = 22300$ were observed when the non-dimensionalised mass-damping factor becomes 0.314 and 1.04 respectively.

A contradictory behaviour is observed at low m^* between the low and high Re cases. The forcing due to vortex shedding at low Reynolds numbers suppresses the galloping excitation and results in a reduced power output. For the case with high Re power output increases as m^* is reduced . For this high Re case, at low m^* the reduction in inertia allows the body to accelerate faster and spend a larger portion of the period at relatively high transverse velocities. Extrapolating this trend, the limit to peak efficiency is found to be 13.5% and occurs when $m^* \to 0$ and $U^* \to \infty$ and $\Pi_2 = 1.22$

Keywords:

1. Introduction

The search for alternate energy sources with minimal environmental impact has become an important area of research in the modern word. Solar, wind power and wave power are some of the examples of these sources. Recently, a new branch of research has been developing to extract energy from flow induced vibrations (Bernitsas et al., 2008). It has been hypothesized that this technique may work efficiently in areas where regular turbines cannot.

An elastically-mounted slender structure such as a cylinder which is susceptible to flow-induced vibrations has the potential for energy extraction. With regards to slender bodies, two common types of flow-induced vibrations are vortex-induced vibrations (VIV) and aeroelastic galloping. Significant research has been carried out by Bernitsas and his team on extracting useful energy from VIV. Some of their significant work includes investigating the influence of physical parameters such as mass ratio, Reynolds number, mechanical properties (Raghavan and Bernitsas, 2011; Lee and Bernitsas, 2011) and the influence of the proximity of a solid boundary (Raghavan et al., 2009). However, the possibility of extracting energy using aeroelastic galloping has not been thoroughly investigated. Some theoretical work was carried out by Barrero-Gil et al. (2010). Utilizing galloping may be a more viable method to harness energy from flow-induced vibrations as it is not bounded by a narrow "lock-in" range of reduced velocities (U^*). This study further explores the possibility of harnessing energy from flow induced vibrations using aeroelastic galloping.

According to Païdoussis et al. (2010), Glauert (1919) provided a criterion for galloping by considering the auto-rotation of an aerofoil. Den Hartog (1956) provided a theoretical explanation for galloping for iced electric transmission lines. A weakly non-linear theoretical aeroelastic model to predict the response of galloping was developed by Parkinson and Smith (1964) based on the quasi-steady state (QSS) theory. Experimental lift and drag data on a fixed square prism at different angles of attack were used as an input for the theoretical model. It essentially used a curve fit of the transverse force to predict the galloping response. The study managed to achieve a good agreement with experimental data.

However, the QSS model equation when solved analytically using the sinusoidal solution method cannot predict the response for cases with low mass ratios. Joly et al. (2012) observed that finite element simulations show a sudden change in amplitude below a critical value of the mass ratio. The model equation defined in Parkinson and Smith (1964) was modified to account for the vortex shedding and solved numerically to predict the reduced amplitude at low mass ratios to the point where galloping is no longer present. Barrero-Gil et al. (2010) investigated the possibility of extracting power from vibrations caused by galloping using the quasi-steady state model. In the conclusions of that paper it was pointed out that in order to obtain a high power to area ratio, the mass-damping ($m^*\zeta$) parameter should be kept low. The same study investigated the influence of the characteristics of the C_y curve on maximum power output.

Here, the modified QSS model developed by Joly et al. (2012) is integrated numerically for low Reynolds numbers. The focus is on the power extraction potential as a function of mechanical parameters (i.e. frequency of oscillation, damping factor and mass ratio). To this end, a series of previously mentioned mechanical parameters are tested at two different values of Re: $Re = 165$, a case that should remain laminar and essentially two-dimensional; $Re = 22300$, a case where the flow is expected to be turbulent and three-dimensional. Both cases require the input of transverse force coefficients C_y as a function of angle of attack θ for a fixed body. These data are provided from direct numerical simulations for the $Re = 165$ case, while the data provided by Parkinson and Smith (1964) are used for the $Re = 22300$ case.

The structure of the paper is as follows. Section 2 presents the modified QSS model, the method for the calculation of power output, and the parameters used. Section **??** presents the results, first of the fixed body tests at a range of θ, then of the response characteristics predicted by the integration of the QSS model for both the high and low Re cases. For the low Re case, the results of the QSS model are compared to those of full direct numerical simulations of the fluid-structure interaction problem. Finally, section **??** presents the conclusions that can be drawn from this work.

Nomenclature

a_1, a_3, a_5, a_7	coefficients of the polynomial to determine C_y
A	displacement amplitude
c	damping constant
D	characteristic length (side length) of the cross section of the body
$f = \sqrt{k/m}/2\pi$	natural frequency of the system
F_y	instantaneous force normal to the flow
F_0	amplitude of the oscillatory force due to vortex shedding
k	spring constant
m	mass of the body
m_a	added mass
P_d	power dissipated due to mechanical damping
$P_{in} = \rho U^3 D/2$	Energy flux of the approaching flow
P_{mean}	mean power
P_t	power transferred to the body by the fluid
t	time
U	freestream velocity
U_i	Induced velocity
$y, \dot{y}, \ddot{y}$	transverse displacement, velocity and acceleration of the body
$\mathcal{A} = DL$	frontal area of the body
λ	Inverse time scale of a galloping dominated flow
$\lambda_{1,2}$	Eigenvalues of linearized equation of motion
ρ	fluid density
$\omega_n = 2\pi f$	natural angular frequency of the system
ω_s	vortex shedding angular frequency
$c^* = cD/mU$	non-dimensionalised damping factor
$C_y = F_y/0.5\rho U^2 DL$	normal (lift) force coefficient
$m^* = m/\rho D^2 L$	mass ratio
Re	Reynolds number
$U^* = U/fD$	reduced velocity
$Y = y/D$	non-dimensional transverse displacement
$\dot{Y} = m^* \dot{y}/a_1 U$	non-dimensional transverse velocity
$\ddot{Y} = m^{*2} D/a_1^2 U^2$	non-dimensional transverse acceleration
$\Gamma_1 = 4\pi^2 m^{*2}/U^{*2} a_1^2$	First dimensionless group arising from linearised, non-dimensionalised equat
$\Gamma_2 = c^* m^*/a_1$	Second dimensionless group arising from linearised, non-dimensionalised equ
$\zeta = c/2m\omega_n$	damping ratio
$\theta = \tan^{-1}(\dot{y}/U)$	instantaneous angle of incidence (angle of attack)
$\Pi_1 = 4\pi^2 m^{*2}/U^{*2}$	Combined mass-stiffness parameter
$\Pi_2 = c^* m^*$	Combined mass-damping parameter

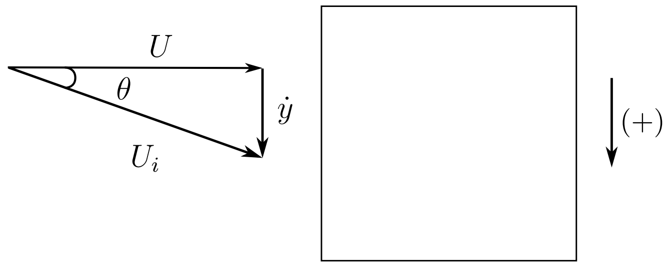

Figure 1: Induced angle of attack on the square prism due to the resultant of free-stream velocity of the fluid and transverse velocity of the body.

2. Problem formulation and methodology

2.1. The quasi-steady state (QSS) model

The base quasi-steady state (QSS) model was first developed by Parkinson and Smith (1964) for a square cross section. The equation of motion of the body is given by

$$(m + m_a)\ddot{y} + c\dot{y} + ky = F_y, \tag{1}$$

where the forcing term F_y is given by

$$F_y = \frac{1}{2}\rho U^2 \mathcal{A} C_y. \tag{2}$$

Lighthill (1986) showed that for systems oscillating in fluid, it is sometimes useful to decompose the fluid forces into components that are in and out of phase with the body acceleration. The component in phase with the acceleration effectively adds to the inertia or effective mass of the system. Therefore, an added mass term, m_a, can be added to the system mass. For consistency with previous studies such as Joly et al. (2012), a value of $m_a = 3.5$ has been used here.

In the QSS model, it is assumed that the force on the body at a given instantaneous incident angle θ (defined in figure 1) is the same as the mean force on a static body at the same incident angle, or angle of attack. The instantaneous value of C_y is therefore determined by an interpolating polynomial based on the lift data for flow over a stationary body at various θ. Using the relationship between θ and the instantaneous transverse velocity of the body $\dot{y}$ shown in figure 1, C_y can be written as a function of $\dot{y}$. The order of the interpolation polynomial used to define this function has varied from study to study. For example a 7^{th} order polynomial was used in Parkinson and Smith (1964) and 3^{rd} order polynomial was used in Barrero-Gil et al. (2009). Ng et al. (2005) concluded that using a 7^{th} order polynomial is sufficient and a polynomial higher than that of 7^{th} order doesn't provides a significantly better result. Thus a 7^{th} order interpolating polynomial is used in this present study. As a result, $C_y(\theta)$ (noting that theta is proportional to $\dot{y}/U$) is defined as

$$C_y(\theta) = a_1\left(\frac{\dot{y}}{U}\right) + a_3\left(\frac{\dot{y}}{U}\right)^3 + a_5\left(\frac{\dot{y}}{U}\right)^5 + a_7\left(\frac{\dot{y}}{U}\right)^7. \tag{3}$$

It is expected that vortex shedding will be well correlated along the span and provide significant forcing at low Re. Joly et al. (2012) introduced an additional sinusoidal forcing function to the hydrodynamic forcing to model this. This enables the model to provide accurate predictions even at low mass ratios where galloping excitation is suppressed or not present. In this study, the forcing due to vortex shedding in low Re cases is incorporated using a sinusoidal forcing function $F_0 \sin \omega_s t$ added to the right-hand side of equation 1. Here, ω_s and F_0 represent the angular vortex shedding frequency and the maximum force due to shedding respectively. Thus, the final equation for the modified QSS model is

$$m\ddot{y}+c\dot{y}+ky=\frac{1}{2}\rho U^2\mathcal{A}\left(a_1\left(\frac{\dot{y}}{U}\right)+a_3\left(\frac{\dot{y}}{U}\right)^3+a_5\left(\frac{\dot{y}}{U}\right)^5+a_7\left(\frac{\dot{y}}{U}\right)^7\right)+F_0\sin{(\omega_s t)}. \quad (4)$$

This equation can be solved using standard time integration methods. In this study the fourth-order Runge-Kutta scheme built in to the MATLAB routine 'ode45' was generally used to obtain the solutions. Some low mass ratio cases used a solver modified for stiff problems, built into the 'ode15s' routine in MATLAB.

2.2. Calculation of average power

The dissipated power due to the mechanical damping represents the ideal potential amount of harvested power output. Therefore, the mean power output can be given by

$$P_{mean} = \frac{1}{T}\int_0^T (c\dot{y})\dot{y}dt, \quad (5)$$

where T is the period of integration and c is the mechanical damping constant.

It should be noted that this quantity is equal to the work done on the body by the fluid, defined as

$$P_{mean} = \frac{1}{T}\int_0^T F_y\dot{y}dt, \quad (6)$$

where F_y is the transverse (lift) force.

These two definitions show two important interpretions of the power with respect to any energy production device. The first shows that power will be high for situations where the damping coefficient is high, and the transverse velocity is consistently high. The second shows that power will be high for situations where the transverse force and the body velocity are in phase.

2.3. Parameters used

For the low Re tests, $Re = 165$ was maintained as it was pointed out by Sheard et al. (2009) and Tong et al. (2008) that the three-dimensional transition for a square cylinder occurs at approximately Re=160. F_0 was kept at 0.4937 which was obtained by scaling the value used by Joly et al. (2012) with the amplitude ratios of the lift forces obtained at the different Reynolds numbers.

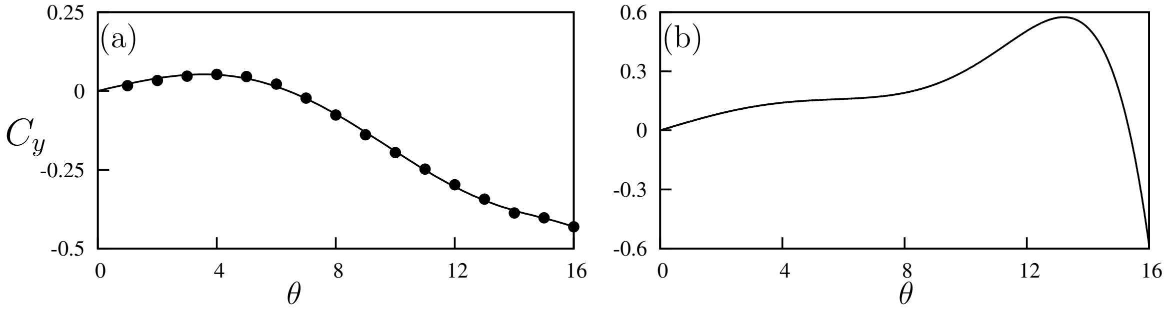

Figure 2: Lift coefficient, C_y, as a function of incidence angle θ, for a static square cross section. (a) Data from simulations at Re = 165 (b) data from Parkinson and Smith (1964) at Re = 22300. Points (•) are measurements from the simulations. The solid lines in both plots are 7th-order interpolating polynomial used to predict the fluid forcing for the QSS model. C_y is the force coefficient of the force which occurs normal to the induced velocity.

Case	a_1	a_3	a_5	a_7
Re=165	1.3	125.3	1825.73	8765.3
Re=22300	2.69	168	1670	59900

Table 1: Coefficient values used in the 7th order interpolation polynomial for high (Re = 22300) and low (Re = 165) Reynolds numbers. These data are used as input data to calculate the right-hand side of Eq. 4 throughout this study.

The angular vortex shedding frequency ω_s, was set to 0.98 which was obtained by performing a power spectral analysis of the stationary data at 0°. Stationary C_y data were obtained at different angles of attack ranging from 0° to 16°. The average power was obtained by using equation 5, and the averaging was done over no less than 20 galloping periods. Predictions of power output at Re = 22300 were obtained using the coefficients for curve fitting C_y (Table (1)) from Parkinson and Smith (1964), in order to provide a comparison between high and low Reynolds numbers. The mass ratio m^* was kept at 1163 for Re = 22300 (Similar to Parkinson and Smith (1964)) and m^* = 20 for Re=165. These parameters were used throughout this study unless otherwise specified.

The stationary data and the fluid-structure interaction (FSI) data were obtained using a high-order spectral element routine to simulate the two-dimensional laminar flow. Simulations involving fluid structure interaction (FSI) were used to provide additional validation of the QSS model. The inlet was placed $20D$ while the outlet situated $60D$ away from the centroid of the body. The side boundaries were placed $20D$ away from the centroid of the body where D was kept as unity throughout this study. The Navier–Stokes equations were solved in an accelerated frame of reference attached to the moving body along with the body equation of motion given in equation 1. A three-step time splitting scheme together with high-order Lagrangian polynomials were used to obtain the solution. The details of the method can be found in Thompson et al. (2006, 1996). This code has been very well validated in a variety of fluid-structure interaction problems (Leontini et al., 2007; Griffith et al., 2011; Leontini et al., 2011; Leontini and Thompson, 2013).

The computational domain consists of 690 quadrilateral macro elements where the majority of the elements were concentrated near the square section. A freestream condition was given to the inlet, top and bottom boundaries and the normal velocity gradient was set to zero at the outlet. A convergence study was performed by changing the order of the polynomial (p-refinement) at $U^* = 40$ and $Re = 165$. A 9^{th} order polynomial together with a time step of $\Delta t U/D = 0.001$ was sufficient to ensure an accuracy of 2% with regards to amplitude of oscillation.

Barrero-Gil, A., Alonso, G., Sanz-Andres, A., Jul. 2010. Energy harvesting from transverse galloping. Journal of Sound and Vibration 329 (14), 2873–2883.

Barrero-Gil, A., Sanz-Andrés, A., Roura, M., Oct. 2009. Transverse galloping at low Reynolds numbers. Journal of Fluids and Structures 25 (7), 1236–1242.

Bernitsas, M. M., Raghavan, K., Ben-Simon, Y., Garcia, E. M. H., 2008. VIVACE (Vortex Induced Vibration Aquatic Clean Energy): A new concept in generation of clean and renewable energy from fluid flow. Journal of Offshore Mechanics and Arctic Engineering 130 (4), 041101–15.

Den Hartog, J. P., 1956. Mechanical Vibrations. Dover Books on Engineering. Dover Publications.

Glauert, H., 1919. The rotation of an aerofoil about a fixed axis. Tech. rep., Advisory Committee on Aeronautics R and M 595. HMSO, London.

Griffith, M. D., Leontini, J. S., Thompson, M. C., Hourigan, K., 2011. Vortex shedding and three-dimensional behaviour of flow past a cylinder confined in a channel. Journal of Fluids and Structures 27 (5-6), 855–860.

Joly, A., Etienne, S., Pelletier, D., Jan. 2012. Galloping of square cylinders in cross-flow at low Reynolds numbers. Journal of Fluids and Structures 28, 232–243.

Lee, J., Bernitsas, M., Nov. 2011. High-damping, high-Reynolds VIV tests for energy harnessing using the VIVACE converter. Ocean Engineering 38 (16), 1697–1712.

Leontini, J. S., Lo Jacono, D., Thompson, M. C., Nov. 2011. A numerical study of an inline oscillating cylinder in a free stream. Journal of Fluid Mechanics 688, 551–568.

Leontini, J. S., Thompson, M. C., 2013. Vortex-induced vibrations of a diamond cross-section: Sensitivity to corner sharpness. Journal of Fluids and Structures 39, 371–390.

Leontini, J. S., Thompson, M. C., Hourigan, K., Apr. 2007. Three-dimensional transition in the wake of a transversely oscillating cylinder. Journal of Fluid Mechanics 577, 79.

Lighthill, J., 1986. Fundamentals concerning wave loading on offshore structures. Journal of Fluid Mechanics 173, 667–681.

Ng, Y., Luo, S., Chew, Y., Jan. 2005. On using high-order polynomial curve fits in the quasi-steady theory for square-cylinder galloping. Journal of Fluids and Structures 20 (1), 141–146.

Païdoussis, M., Price, S., de Langre, E., 2010. Fluid-Structure Interactions : Cross-Flow-Induced Instabilities. Cambridge University Press.

Parkinson, G. V., Smith, J. D., 1964. The square prism as an aeroelastic non-linear oscillator. The Quarterly Journal of Mechanics and Applied Mathematics 17 (2), 225–239.

Raghavan, K., Bernitsas, M., Apr. 2011. Experimental investigation of Reynolds number effect on vortex induced vibration of rigid circular cylinder on elastic supports. Ocean Engineering 38 (5-6), 719–731.

Raghavan, K., Bernitsas, M. M., Maroulis, D. E., 2009. Effect of Bottom Boundary on VIV for Energy Harnessing at $8 \times 10^3 < Re < 1.5 \times 10^5$. Journal of Offshore Mechanics and Arctic Engineering 131 (3), 031102.

Sheard, G. J., Fitxgerald, M. J., Ryan, K., Jun. 2009. Cylinders with square cross-section: wake instabilities with incidence angle variation. Journal of Fluid Mechanics 630, 43.

Thompson, M., Hourigan, K., Sheridan, J., Feb. 1996. Three-dimensional instabilities in the wake of a circular cylinder. Experimental Thermal and Fluid Science 12 (2), 190–196.

Thompson, M. C., Hourigan, K., Cheung, A., Leweke, T., Nov. 2006. Hydrodynamics of a particle impact on a wall. Applied Mathematical Modelling 30 (11), 1356–1369.

Tong, X., Luo, S., Khoo, B., Oct. 2008. Transition phenomena in the wake of an inclined square cylinder. Journal of Fluids and Structures 24 (7), 994–1005.